Two-step photocurrent generation enhanced by miniband formation in InAs/GaAs quantum dot superlattice intermediate-band solar cells

Watanabe, Sho ; Asahi, Shigeo ; Kada, Tomoyuki ; Hirao, Kazuki ; Kaizu, Toshiyuki ; Harada, Yukihiro ; Kita, Takashi

(Citation)
Applied Physics Letters,110(19):193104-193104

(Issue Date)
2017-05-08

(Resource Type)
journal article

(Version)
Version of Record

Two-step photocurrent generation enhanced by miniband formation in InAs/GaAs quantum dot superlattice intermediate-band solar cells

Sho Watanabe, Shigeo Asahi, Tomoyuki Kada, Kazuki Hirao, Toshiyuki Kaizu, Yukihiro Harada, and Takashi Kita

Citation: Appl. Phys. Lett. **110**, 193104 (2017); doi: 10.1063/1.4983288
View online: http://dx.doi.org/10.1063/1.4983288
View Table of Contents: http://aip.scitation.org/toc/apl/110/19
Published by the American Institute of Physics

Two-step photocurrent generation enhanced by miniband formation in InAs/GaAs quantum dot superlattice intermediate-band solar cells

Sho Watanabe, Shigeo Asahi, Tomoyuki Kada, Kazuki Hirao, Toshiyuki Kaizu, Yukihiro Harada, and Takashi Kita
Department of Electrical and Electronic Engineering, Graduate School of Engineering, Kobe University, 1-1 Rokkodai, Nada, Kobe 657-8501, Japan

(Received 25 January 2017; accepted 28 April 2017; published online 11 May 2017)

We studied the effects of miniband formation on the photocurrent generated by two-step intersubband absorption in an intermediate-band solar cell incorporating an InAs/GaAs quantum dot superlattice (QDSL). The two-step photocarrier generation increases with the electronic state coupling of InAs QDSLs in the intrinsic layer. Because carriers that are excited into the superlattice minibands spatially separate in an internal electric field, the electron–hole recombination rate for the photoexcited carriers decreases, and therefore, the electron lifetime increases. The long-lived electrons in the intermediate states of the QDSL miniband increase the intersubband absorption strength. We confirmed a systematic sensitive change in the two-step photocurrent generation depending on the miniband formation controlled by the temperature. *Published by AIP Publishing.* [http://dx.doi.org/10.1063/1.4983288]

Photovoltaics using *p-i-n* semiconductor solar cells (SCs) have been attracting interest in recent years because they are renewable. Generally, as the conversion efficiency of a single-junction SC is reduced by various unavoidable losses, the maximum conversion efficiency is limited to approximately 30% under one sun of illumination and approximately 40% under the maximum concentration of solar irradiance.[1] One of the important losses limiting the conversion efficiency is the transmission loss arising from photons with less energy than the SC bandgap energy. To surpass the single-junction limit, various types of high-efficiency SCs have been proposed. In particular, multijunction SCs consisting of semiconductors with different bandgap energies are one of the promising approaches. The current highest energy conversion efficiency has been attained by four-junction concentrator SCs.[2] Another promising approach is the intermediate band (IB) SC containing an additional parallel diode connection.[3] The intermediate-band solar cell (IBSC) has attracted strong attention because of its extremely high theoretical prediction of conversion efficiency greater than 40% under one sun of irradiation and 60% under the maximum concentration.[4] IBSCs not only enable the efficiency to surpass one of the current best SCs but also robustly operate under a solar spectral variation compared to multijunction SCs.[5]

A typical IBSC with a single band in the bandgap provides two additional sub-bandgap photon absorptions from the valence band (VB) to the IB and from the IB to the conduction band (CB), together with the ordinary interband photon absorption from the VB to the CB. These additional transitions for the sub-bandgap photons produce extra photocurrent without decreasing the photovoltage if electrons in the IB are optically pumped out to the CB.[3,6] Additional photocurrent generation occurs under a current-matched condition, but the intersubband photon absorption from the IB to the CB is generally very weak compared to the interband photon absorption from the VB to the IB due to dipole transition selectivity.[7] The oscillator strength of the intersubband absorption is generally proportional to the electron density in the initial state.[8,9] It is, therefore, necessary to increase the intersubband absorption strength to a level equivalent to the interband absorption by reducing the carrier recombination rate, leading to an extension of the electron lifetime in the IB.[4]

We have studied the enhanced two-step photocarrier generation caused by the effective electron–hole separation in the minibands of quantum dot superlattice (QDSL) structures embedded in the intrinsic layer of *p-i-n* SC structures. By densely stacking quantum dots (QDs), they will be electrically coupled along the stacking direction and, thereby, form minibands.[10] As carriers excited into the minibands can be spatially separated in an internal electric field of an SC, the electron–hole recombination rate can be reduced and the electron lifetime in the miniband can be extended.[11] Although it has been confirmed that long-lived electrons improve the two-step photocurrent generation in QDSLs, it is still unclear how the change in electronic coupling between QDs influences the generation of the two-step photocurrent. In this study, we studied the detailed temperature dependence of the two-step photocurrent generated in InAs/GaAs QDSL-IBSCs and compared the results with the carrier dynamics observed in time-resolved photoluminescence (PL) demonstrating miniband formation.

A QDSL-IBSC structure with a *p-i-n* junction was fabricated on an n^+-GaAs (001) substrate using solid-source molecular beam epitaxy, as shown in Fig. 1. Initially, we grew a 2000-nm-thick *i*-layer incorporating a QDSL structure at 480 °C on an *n*-GaAs (700 nm, Si: 5×10^{17} cm^{-3})/n^+-GaAs (150 nm, Si: 1×10^{18} cm^{-3}) layer grown at 550 °C on the substrate. The undoped *i*-layer structure comprises of GaAs (674 nm), InAs/GaAs QDSLs, and GaAs (1290 nm) layers. The nominal thickness of InAs was 2.1 monolayers (MLs) for forming the first QD layer and 1.4 MLs for the subsequently stacked layers.[10] A small amount of InAs for the stacked layer prevents the lateral size of QDs from

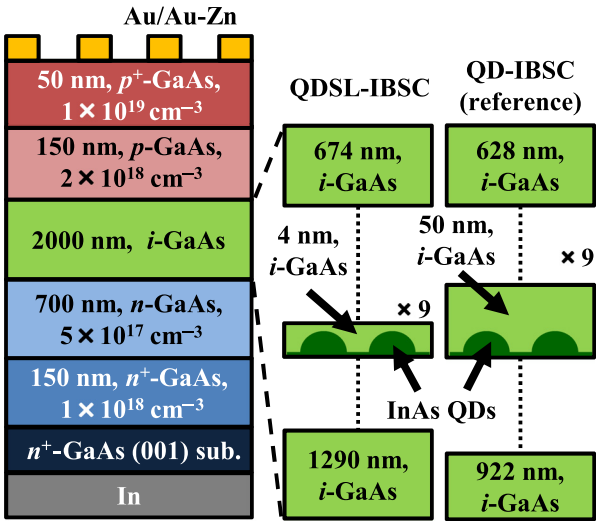

FIG. 1. Schematic sample structures of the InAs/GaAs QDSL-IBSC and QD-IBSC (reference sample). It was fabricated on the GaAs (001) substrate using solid-source molecular beam epitaxy.

expanding. The GaAs spacer layer thickness was 4 nm, which is thin enough to couple the electronic states along the stacking direction and form superlattice (SL) minibands.[10] The SL period was 9. In addition, a p^+-GaAs (50 nm, Be: 1×10^{19} cm^{-3})/p-GaAs (150 nm, Be: 2×10^{18} cm^{-3}) layer was then grown at 500 °C on top of the i layer. The beam equivalent pressure of the As_2 flux during the growth was 1.3×10^{-3} Pa. The metal contacts on the top and bottom surfaces were Au/Au–Zn and In, respectively. The total thickness of the QDSL layer and the in-plane QD density were approximately 38 nm and 1×10^{10} cm^{-2}, respectively. The built-in internal electric field in the intrinsic region of the SC was expected to be 7 kV/cm, which is low enough to prevent electric-field-induced tunneling carrier escape from the QDSL.[12] For reference, we fabricated an InAs/GaAs QD-IBSC (Fig. 1) with the same structure except for the GaAs spacer layer thickness of 50 nm, where the nominal thickness of InAs was 2.1 MLs for all the QD layers. This GaAs spacer layer was sufficiently thick to prevent miniband formation.

In order to confirm the electronic coupling between QDs along the stacking direction, we measured the in-plane linear polarized PL of the QDSL-IBSC and QD-IBSC using a laser diode with a wavelength of 659 nm, which excites electrons from the VB to the CB in GaAs. The excitation power density was 8.0 W/cm^2. Figure 2(a) displays the polarized PL spectra of the QDSL-IBSC at 20 K. Two clear components can be observed in the polarized PL spectra. We performed curve fitting using two Gaussian functions to separate these components. Figure 2(b) presents the fitted results. The PL peak at 1080 nm is isotropic, attributed to the fundamental transition of the electrically isolated, large QDs in the first layer.[10] The peak at 1040 nm indicates a clear polarization anisotropy; the [–110]-polarization component is stronger than the [110]-polarization component.[10,13] This is a typical feature caused by the relaxing of the vertical confinement in QDSLs.[13] The anisotropic signal arises from the fundamental transition in QDSLs.[11] Conversely, the in-plane linear polarized PL of the QD-IBSC shown in Fig. 2(c) is isotropic, whose peak appears at 1100 nm due to the fundamental

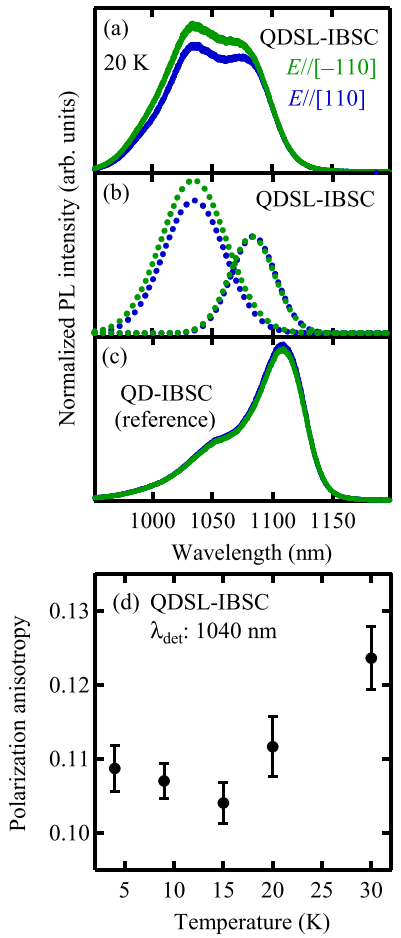

FIG. 2. (a) In-plane linear polarized PL spectra in the QDSL-IBSC at 20 K. (b) Dotted lines indicate the Gaussian fitting curves of the in-plane linear polarized PL spectra. (c) In-plane linear polarized PL spectra in the QD-IBSC at 20 K. (d) Temperature dependence of the polarization anisotropy at the fundamental state of the QDSL-IBSC. The polarization anisotropy is defined as $(I_{[-110]}-I_{[110]})/(I_{[-110]}+I_{[110]})$, where $I_{[-110]}$ and $_{[110]}$ denote the PL intensities polarized along [−110] and [110], respectively.

transition in QDs with a small sideband signal at 1050 nm arising from the excited states. This suggests that electronic coupling along the internal electric field does not occur in the QD-IBSC. Figure 2(d) shows the temperature dependence of the polarization anisotropy at the fundamental states of the QDSL-IBSC. The polarization anisotropy is defined as $(I_{[-110]}-I_{[110]})/(I_{[-110]}+I_{[110]})$, where $I_{[-110]}$ and $I_{[110]}$ are the PL intensities polarized along [−110] and [110], respectively. In this measurement, we used a supercontinuum white laser for the excitation. The excitation wavelength selected by using a 27-cm single monochromator was 800 nm, and the excitation density was 2.9 mW/cm^2. The polarization anisotropy is almost constant in the temperature range below 15 K, suggesting that the electronic coupling length of the fundamental states of QDs is almost unchanged in this temperature range.[13] The gradual increase appeared above ∼20 K indicates that the coupling starts extending along the stacking direction.[10] Utilizing these two SCs, we study the effects of miniband formation on two-step photocurrent generation.

We conducted two-color photoexcitation measurements using two excitation light sources. A light emitting diode with a wavelength of 940 nm and an excitation power density of 2.74×10^{16} photons/cm^2 was utilized for the excitation

between the VB and the excited states in the QDSLs.[11] A continuous-wave infrared laser light with a wavelength of 1550 nm chopped by using an optical chopper ($f = 1$ kHz) was used for the intersubband excitation between the IB and the CB. We recorded a short-circuit photocurrent detected by a lock-in amplifier synchronized with an optical chopper. We define ΔI as the change in photocurrent caused by the intersubband excitation. Here, we measured the dependence of ΔI on temperature in the range from 12 to 280 K. Figure 3 presents the measured ΔI for the QDSL-IBSC and QD-IBSC normalized by each ΔI at 12 K. The two-step photocurrent of the QDSL-IBSC is approximately one order greater than that of the QD-IBSC at 9 K (Fig. 2(c) of Ref. 11). The ΔI of the QDSL-IBSC increases as the temperature rises to 50 K, and then, it saturates and starts decreasing. The decrease in ΔI for the QDSL-IBSC above 50 K and QD-IBSC above 100 K is explained by a decrease in electron density in the IB due to thermal escape. Conversely, the ΔI of the QD-IBSC slightly decreases up to 40 K and subsequently decreases in a complex manner. A hump structure appears around 100 K, which was never observed in the QDSL-IBSC and is a typical feature observed for IBSCs containing uncoupled QDs. This can be attributed to the thermal hole escape from QDs. The valence-band potential barrier height for holes in InAs/GaAs QDs is approximately 120 meV, while the conduction-band potential barrier height for electrons is 270 meV. These are evaluated by the results of the atomistic first principles calculation performed by Yang *et al.*[14] We estimated the thermal carrier escape time as a function of the temperature by using the thermionic emission model derived in Refs. 15 and 16. We modified the model for taking into account the three-dimensional confinement to adapt to QDs. Electrons pumped to the excited state in QDs can escape thermally by two routes. Part of excited electrons directly escape from the excited state before relaxing to the fundamental state.[17] The ΔI of the QD-IBSC starts decreasing above ~40 K owing to the direct thermal escape of electrons from the excited state. The temperature dependence of ΔI shows a dip at ~60 K and is followed by the hump structure. As the thermal escape time for holes shortens with the increasing temperature and becomes comparable to the recombination rate at around 60 K, holes start escaping from QDs above ~60 K. Thereby, the electron lifetime is extended, and ΔI increases.[18] When temperature rises furthermore, electrons in the fundamental state also start escaping, and ΔI substantially decreases.

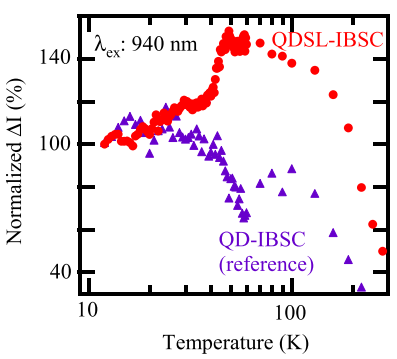

FIG. 3. Comparison of the temperature dependence of normalized ΔI for the QDSL-IBSC and the QD-IBSC in the temperature range of 12 to 280 K.

Such a thermal excitation process can be suppressed by introducing a high potential barrier.[7]

Here, we focus on different features of ΔI observed in the temperature range from 12 to 50 K. The two SC structures exhibit opposite ΔI; the ΔI of the QDSL-IBSC (QD-IBSC) increases (decreases) with temperature. We considered that this arises from the SL structure. When adjacent QD states along the stacked direction are distributed within the homogeneous linewidth, the electronic states can couple and, thereby, form minibands.[10] The homogeneous linewidth of the fundamental and excited states of InGaAs QDs has been reported to be 5–10 μeV and approximately 200 μeV at 4 K, respectively.[19] The homogeneous linewidth of the higher excited states is more than one order of magnitude larger than that of the fundamental states because of the weaker electron confinement in the higher excited states. These linewidths increase rapidly with temperature; for example, the linewidth of the fundamental state of InGaAs QDs increases to approximately 10 meV at room temperature.[20] Thus, the degree of electronic coupling increases with temperature.[10] To investigate the influence of photoexcited carrier dynamics in SL minibands on ΔI, we conducted time-resolved PL measurements for the QDSL-IBSC using a near-infrared streak camera system with a temporal resolution of 20 ps. A mode-locked Ti:sapphire pulse laser with a wavelength of 900 nm was utilized for the interband excitation corresponding to the transition from the VB to the higher excited states of QDSLs.[11] The pulse duration was 140 fs, the repetition rate was 4 MHz, and the excitation power density was 4.5 nJ/cm^2. Figure 4(a) displays the temperature dependence of the time-resolved PL profile of the fundamental transition in QDSLs detected at 1050 nm. Each decay profile follows a double exponential curve. According to our earlier work,[12] this rapid decay component is attributed to the recombination of unseparated electrons and holes at the fundamental state in each QD. Conversely, the slow decay component is due to the electrons and holes spatially separated in the excited-state miniband by the internal electric field. Figure 4(b) summarizes the analyzed decay times of the rapid and slow decay components as a function of temperature. The slow decay time increases with temperature up to 40 K, while the rapid decay time is almost constant in this temperature range. The temperature insensitivity of the rapid decay component indicates that the fundamental state does not sufficiently couple and does not form a miniband in which the excited carriers can be transported because the radiative recombination rate of carriers in uncoupled, three-dimensionally confined QDs is independent of temperature.[21,22] The gradual increase in the slow decay time indicates that the excited carriers are transported along the stacking direction in the miniband.[10] Here, it is noted that the excitation laser with the wavelength of 900 nm excites the higher excited states of the QDSL. The excited carriers are spatially separated in the excited state minibands. As the homogeneous linewidth of the higher excited states is more than one order of magnitude larger than that of the fundamental states,[19] electronic coupling in the higher excited states more easily occurs than that in the fundamental state.[11] When the temperature increases above 40 K, the rapid decay time starts increasing with temperature, while the slow decay

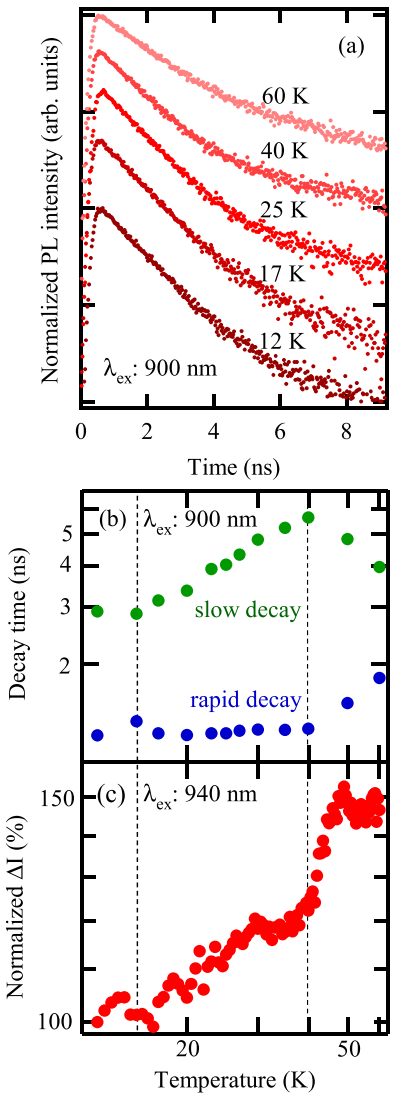

FIG. 4. (a) Temperature dependence of the time-resolved PL intensity from the fundamental transitions for the QDSL-IBSC. (b) Temperature dependence of analyzed decay times for slow and rapid decay components. (c) Temperature dependence of ΔI for the QDSL-IBSC in the temperature range of 12 to 60 K. Dashed lines at 15 K and 40 K represent critical temperatures observed in slow and rapid decay times.

time decreases. This result indicates that the fundamental state miniband starts forming above 40 K. Thus, electrons and holes in the fundamental state are efficiently separated toward the opposite direction along the internal electric field, which extends the recombination lifetime. Quick carrier separation in the fundamental state miniband causes rapid carrier relaxation from the excited states to the unoccupied fundamental state and prevents long-distance carrier separation in the excited state minibands. Consequently, the slow decay component decreases, as shown in Fig. 4(b). Excited electrons and holes are separated along the SL in the internal electric field of the SC, causing an extended, long carrier recombination lifetime, resulting in an enhancement in the intersubband transition strength.

Next, we compare the ΔI of the QDSL-IBSC with the PL decays in the temperature range from 12 to 60 K. The ΔI in Fig. 4(c) increases gradually up to 40 K and exhibits a significant increase above 40 K. The gradual increase in ΔI observed below 40 K coincides with the change in the slow decay component, as shown in Fig. 4(b). Here, the intersubband absorption is enhanced by the extended carrier lifetime caused by the carrier separation in the excited state minibands. The further increase in ΔI observed above 40 K corresponds to the quick and effective carrier separation in the fundamental state miniband. These results demonstrate that two-step photocarrier generation can be dramatically enhanced by extending the electron lifetime in the IB. Here, it is noted that the final state of the first interband excitation is different from the initial state of the second intersubband excitation. This picture agrees well with the concept of a photon ratchet IBSC proposed by Yoshida *et al.*[23]

In summary, we studied the effects of miniband formation on intersubband absorption in IBSCs incorporating InAs/GaAs QDSLs. Closely stacked QDs form a SL structure in which the excited states easily form minibands rather than the fundamental state because of the weaker electron confinement in the higher excited states. With increasing temperature, the homogeneous energy distribution increases, and the electronic coupling along the stacking direction becomes strong. Above 40 K, the fundamental state starts forming a miniband. The excited carriers in the miniband can be spatially separated by the internal electric field. The excited electrons and holes are separated along the SL in the internal electric field of the SC, causing an extended, long carrier recombination lifetime and an enhancement in the intersubband transition strength. Two-step photocarrier generation is strictly limited by the intersubband transition and, therefore, dramatically changes with the miniband formation depending on the temperature. In particular, the miniband formation of the fundamental state drastically improves the two-step photocarrier generation. These results demonstrate that two-step photocarrier generation can be dramatically enhanced by extending the electron lifetime in the IB.

This work was partially supported by the Incorporated Administrative Agency New Energy and Industrial Technology Development Organization (NEDO) and the Japan Society for the Promotion of Science (JSPS) KAKENHI under Grant No. JP15K13953.

[1]W. Shockley and H. J. Queisser, J. Appl. Phys. **32**, 510 (1961).
[2]M. A. Green, K. Emery, Y. Hishikawa, W. Warta, E. D. Dunlop, D. H. Levi, and A. W. Y. Ho-Baillie, Prog. Photovoltaics **25**, 3 (2017).
[3]A. Luque and A. Martí, Phys. Rev. Lett. **78**, 5014 (1997).
[4]Y. Okada, N. Ekins-Daukes, T. Kita, R. Tamaki, M. Yoshida, A. Pusch, O. Hess, C. Phillips, D. Farrell, K. Yoshida, N. Ahsan, Y. Shoji, T. Sogabe, and J.-F. Guillemoles, Appl. Phys. Rev. **2**, 021302 (2015).
[5]T. Trupke and P. Würfel, J. Appl. Phys. **96**, 2347 (2004).
[6]A. Luque, J. Appl. Phys. **110**, 031301 (2011).
[7]S. Asahi, H. Teranishi, N. Kasamatsu, T. Kada, T. Kaizu, and T. Kita, J. Appl. Phys. **116**, 063510 (2014).
[8]K. Yoshida, Y. Okada, and N. Sano, Appl. Phys. Lett. **97**, 133503 (2010).
[9]W. G. Hu, T. Inoue, O. Kojima, and T. Kita, Appl. Phys. Lett. **97**, 193106 (2010).
[10]A. Takahashi, T. Ueda, Y. Bessho, Y. Harada, T. Kita, E. Taguchi, and H. Yasuda, Phys. Rev. B **87**, 235323 (2013).
[11]T. Kada, S. Asahi, T. Kaizu, Y. Harada, T. Kita, R. Tamaki, Y. Okada, and K. Miyano, Phys. Rev. B **91**, 201303 (2015).
[12]N. Kasamatsu, T. Kada, A. Hasegawa, Y. Harada, and T. Kita, J. Appl. Phys. **115**, 083510 (2014).
[13]Y. Ikeuchi, T. Inoue, M. Asada, Y. Harada, T. Kita, E. Taguchi, and H. Yasuda, Appl. Phys. Express **4**, 062001 (2011).

[14]X.-F. Yang, X.-S. Chen, W. Lu, and Y. Fu, Nanoscale Res. Lett. **3**, 534 (2008).
[15]H. Schneider and K. V. Klitzing, Phys. Rev. B **38**, 6160 (1988).
[16]D. J. Moss, T. Ido, and H. Sano, IEEE J. Quantum Electron. **30**, 1015 (1994).
[17]K. Hirao, S. Watanabe, S. Asahi, T. Kaizu, Y. Harada, and T. Kita, "Efficient two-step photocurrent in intermediate band solar cells using a highly homogeneous InAs/GaAs quantum-dot superlattice," (unpublished).
[18]S. Asahi, H. Teranishi, N. Kasamatsu, T. Kada, T. Kaizu, and T. Kita, IEEE J. Photovoltaics **6**, 465 (2016).
[19]S. Seidl, M. Kroner, C. Lux, A. W. Holleitner, K. Karrai, R. J. Warburton, A. Badolato, and P. M. Petroff, Appl. Phys. Lett. **92**, 153103 (2008).
[20]M. Sugawara, K. Mukai, Y. Nakata, H. Ishikawa, and A. Sakamoto, Phys. Rev. B **61**, 7595 (2000).
[21]G. Wang, S. Fafard, D. Leonard, J. E. Bowers, J. L. Merz, and P. M. Petroff, Appl. Phys. Lett. **64**, 2815 (1994).
[22]H. Yu, S. Lycett, C. Roberts, and R. Murray, Appl. Phys. Lett. **69**, 4087 (1996).
[23]M. Yoshida, N. J. Ekins-Daukes, D. J. Farrell, and C. C. Phillips, Appl. Phys. Lett. **100**, 263902 (2012).